



## NOTE

## Vessel network formation in response to intermittent hypoxia is frequency dependent

Seema M. Ehsan<sup>1,2</sup> and Steven C. George<sup>1,2,3,4,\*</sup>

<sup>1</sup>Chemical Engineering and Materials Science, University of California, 916 Engineering Tower, Irvine, CA 92697, USA,  
<sup>2</sup>The Edwards Lifesciences Center for Advanced Cardiovascular Technology, University of California, 2400 Engineering Hall, Irvine, CA 92697, USA,  
<sup>3</sup>Biomedical Engineering, University of California, 3120 Natural Sciences II, Irvine, CA 92697, USA,  
<sup>4</sup>and Department of Medicine, University of California, 333 City Blvd. West, Suite 400, Orange, CA 92868, USA<sup>4</sup>

Received 10 September 2014; accepted 15 January 2015

Available online xxx

**A combined experimental and mathematical model of intermittent hypoxia (IH) conditioned engineered tissue was used to characterize the effects of IH on the formation of *in vitro* vascular networks. Results showed that the frequency of hypoxic oscillations has pronounced influence on the vascular response of endothelial cells and fibroblasts.**

© 2015, The Society for Biotechnology, Japan. All rights reserved.

[Key words: Endothelial cells; Vasculogenesis; Oxygen; Intermittent hypoxia; 3D culture; Vascular endothelial growth factor]

Oxygen tension is a key regulator in the angiogenic process required for sustained tumor growth (1). While universal to all solid tumors, this process is inefficient, leading to the presence of both chronic hypoxia (CH; sustained low levels of oxygen) and intermittent hypoxia (IH; the periodic cycling between hypoxia and normoxia). The effects of IH on vascular development are poorly understood, due in large part to the difficulties of controlling dynamic oxygen conditions (2). Furthermore, the kinetics of IH measured *in vivo* varies significantly, spanning frequencies on the order of minutes to days per cycle (3), and fluctuating across tumors as well as within the same tumor (4). Of particular interest is the response of the endothelial lining of tumor blood vasculature, considering the critical role of angiogenesis in tumor progression, and the fact that endothelial cells in normal (non-cancerous) tissue rarely experience hypoxia. Relatively little is known about how IH modulates endothelial cell function, although some reports suggest that IH may protect endothelial cells against apoptosis (5,6), or even render them radioresistant (7). In this note, we investigate the capacity of endothelial cells to form new vasculature structures during IH. We describe a combined experimental and mathematical model of thick, engineered tissue exposed to IH, and use this model to characterize the effects of IH on the formation of vascular networks *in vitro*.

A multi-chambered oxygen control system (Fig. 1A) was fabricated out of polymethyl methacrylate (PMMA) and housed in a 37°C incubator. The LabVIEW controlled system cycles premixed gases containing 1% O<sub>2</sub>, 5% CO<sub>2</sub>, 94% N<sub>2</sub> (C<sub>O<sub>2</sub>, low</sub>) and 20% O<sub>2</sub>, 5% CO<sub>2</sub>,

75% N<sub>2</sub> (C<sub>O<sub>2</sub>, high</sub>). A dynamic fluorescence quenching-based oxygen sensor system (PreSens, Germany) was used to monitor real-time oxygen levels within each chamber.

Endothelial colony forming cell-derived endothelial cells (ECFC-EC) were isolated from human umbilical cord blood as previously described (8), and fed with Endothelial Growth Medium-2 (EGM-2; Lonza, Walkersfield, MD, USA). Normal human lung fibroblasts (NHLF; Lonza) were cultured in Fibroblast Growth Medium-2 (FGM-2; Lonza). 1 × 10<sup>6</sup> ECFC-EC/mL and 2 × 10<sup>6</sup> NHLF/mL were suspended in a fibrinogen solution (10 mg/mL; Sigma–Aldrich, St. Louis, MO, USA), mixed with thrombin (50 units/mL; Sigma–Aldrich), and pipetted onto a circular glass cover slip with an affixed polydimethylsiloxane (PDMS) retaining ring as previously described (9). The rings have a diameter of 8 mm and a height of 0.8 mm, for a final tissue thickness of ~1 mm. Tissues were first maintained at 20% O<sub>2</sub> for 24 h, and then transferred to the desired oxygen condition for an additional 7 days. Supernatant was collected from the tissues on Days 1, 3, 5, and 7 and analyzed for human VEGF-A protein production using ELISA (R&D Systems, Minneapolis, MN, USA).

Tissues were fixed in 10% formalin, blocked with a 2% BSA (Sigma–Aldrich) and 0.1% Tween 20 (Sigma–Aldrich) solution, and incubated with 1:200 mouse anti-human CD31 antibody (Dako, Carpinteria, CA, USA) followed by 1:500 Alexa Fluor 555-conjugated goat anti-mouse IgG (Invitrogen, Carlsbad, CA, USA). Vessels were analyzed using AngioTool (10). 5 random locations were analyzed in each of 9 tissues (*n* = 45) per experimental condition. Statistical comparisons were performed using one-way analysis of variance (ANOVA).

Fick's second law was used to describe the mass balance of oxygen within the media and tissue domains (Fig. 1B), assuming net diffusion in the z-direction only:

\* Corresponding author at: Washington University in St. Louis, 1 Brookings Drive, Campus Box 1097, St. Louis, MO 63130, USA. Tel.: +1 (314) 935 4588; fax: +1 (314) 935 7448.

E-mail address: scg@wustl.edu (S.C. George).

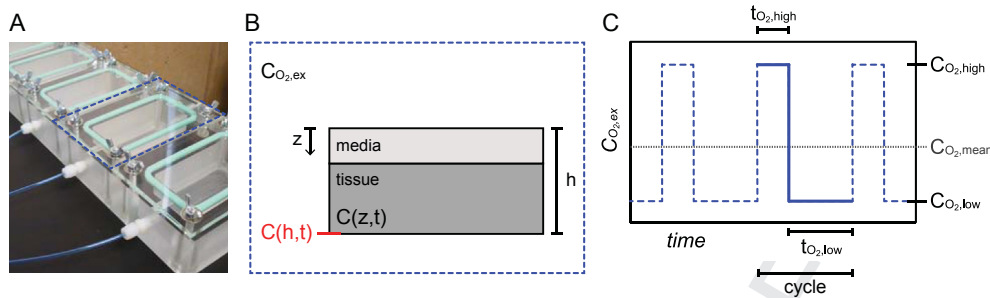


FIG. 1. (A) The fabricated temporal oxygen control system facilitates *in vivo*-like IH dynamics. The blue dotted line outlines a single incubation chamber. (B) Each chamber may be subjected to an external oxygen profile,  $C_{O_2,ex}$ , which is applied to the  $z = 0$  boundary of the media/tissue assembly that is housed inside. (C) A representative IH profile shown by the blue dotted line is characterized by the cycling between  $C_{O_2,high}$  for  $t_{O_2,high}$  and  $C_{O_2,low}$  for  $t_{O_2,low}$ , with a mean oxygen level of  $C_{O_2,mean}$ . The blue solid line segment represents a single cycle. (For interpretation of the references to color in this figure legend, the reader is referred to the web version of this article.)

$$\frac{\partial C_{media}(z,t)}{\partial t} = D_{media} \frac{\partial^2 C_{media}(z,t)}{\partial z^2} \quad \text{Eq. 1}$$

$$\frac{\partial C(z,t)}{\partial t} = D_{tissue} \frac{\partial^2 C(z,t)}{\partial z^2} + \rho_{cell} \frac{V_{max} \cdot C(z,t)}{K_m + C(z,t)} \quad \text{Eq. 2}$$

where  $C_{media}(z,t)$  and  $C(z,t)$  (mol  $O_2/m^3$ , or %  $O_2$ ) are the concentrations of oxygen in the media and tissue domains, respectively, and  $D_{media}$  and  $D_{tissue}$  ( $m^2/s$ ) are the molecular diffusion coefficients of oxygen in the media and tissue domains. The cellular oxygen consumption rate (mol  $O_2 m^{-3} s^{-1}$ ) in the tissue domain was assumed to follow Michaelis–Menten kinetics where  $\rho_{cell}$  (cells/ $m^3$ ) is the volumetric cell density,  $V_{max}$  (mol cell $^{-1} s^{-1}$ ) is the maximum rate of oxygen consumption, and  $K_m$  (mol/ $m^3$ ) is the concentration at which the oxygen consumption rate is half that of  $V_{max}$ . Values used for the parameters  $D_{media}$ ,  $D_{tissue}$ ,  $V_{max}$  and  $K_m$  were  $3.0 \times 10^{-9} m^2/s$ ,  $1.7 \times 10^{-9} m^2/s$ ,  $3.6 \times 10^{-5} mol/m^3/s$  and  $8.0 \times 10^{-3} mol/m^3$ , respectively (11).

No flux boundary conditions were used except for the  $z = 0$  boundary, which was exposed to the externally applied time-varying oxygen profile  $C_{O_2,ex}$ . 20%  $O_2$  was used for initial conditions. The model was solved using the COMSOL Multiphysics time-dependent solver for non-steady state analysis within the built-in module for diffusion-reaction equations. An interpolation function was defined for each time varying boundary condition.

Our fabricated oxygen control system has a 90% response time to a 20%–1%  $O_2$  step change of <30 s, which contrasts sharply with commercially available incubators (e.g., Eppendorf Galaxy 48R) that approach 30 min (data not shown). Thus, our system may facilitate rapid and precise fluctuations in oxygen, which enables comprehensive evaluation of IH with temporal dynamics (Fig. 1C) at the scale of minutes.

Most cells *in vivo* experience normoxia levels of ~5%  $O_2$ , and hypoxia as levels approach ~2%  $O_2$  (12), but are adapted to *in vitro* culture under hyperoxic conditions (~20%  $O_2$ ). Thus, our strategy for IH was to oscillate between 20% and 1%  $O_2$ , representing a high and low ( $C_{O_2,high}$  and  $C_{O_2,low}$ , respectively) value, yet maintain a mean oxygen level ( $C_{O_2,mean}$ ) of 5%  $O_2$ . This strategy would ensure a periodic decrease below 2%  $O_2$ , but maintain a  $C_{O_2,mean}$  consistent with normoxia. We explored a range of IH frequencies consistent with those observed *in vivo* (Table 1). Here, we describe “frequency” as the number of cycles per hour, where a cycle is defined as the sum of  $t_{O_2,high}$  and  $t_{O_2,low}$  (the time at  $C_{O_2,high}$  and  $C_{O_2,low}$ , respectively), or the solid blue line segment in Fig. 1C.

To our knowledge, there are currently no published mathematical models that characterize the response of 3D cellularized tissues subjected to dynamic and/or periodic oxygen conditions (our previous efforts have focused on single step changes in oxygen (11)). We therefore created a non-steady state diffusion-reaction

model with time-varying boundary conditions, and used finite element simulations to predict the resulting oxygen distribution (Fig. 2A). The notable difference between the oxygen profile imposed at the  $z = 0$  boundary ( $C(0,t)$ ; black line in Fig. 2A), and the oxygen profile at the base of the tissue ( $C(h,t)$ ; red line in Fig. 2A) demonstrates the attenuation in transport due to diffusion and cellular consumption. Furthermore, it confirms that for each IH condition, oxygen levels decreased enough during the  $t_{O_2,low}$  intervals to be considered hypoxic. Finally, we used our model to predict  $C_{O_2,mean}$  and found that all IH conditions were within 14% of the 5%  $O_2$  control condition (data not shown).

We next used our system to examine the effects of IH on the potential of endothelial cells to form vessel networks *in vitro*. Interestingly, we found that most IH conditions demonstrated greater vessel development compared to the constant 5%  $O_2$  control, despite having similar  $C_{O_2,mean}$ . Thus, endothelial cells are sensitive to the temporal frequency at which oxygen is delivered. Specifically, we observed a bell-shaped response, with IH 4 (frequency equal to 0.06  $h^{-1}$ ) demonstrating the most pronounced vascular enhancement (Fig. 2B,C).

Blood vessel formation is mediated by hypoxia inducible factor-1 (HIF-1) regulated stromal expression of pro-angiogenic proteins such as vascular endothelial growth factor (VEGF). To investigate if the observed vascular response was related to VEGF production (primarily by the NHLF), we measured the total (accumulated) concentration of VEGF over the 7-day assay. We similarly found that VEGF production is sensitive to the temporal frequency at which oxygen is delivered (Fig. 2D), and further observed an analogous bell-shaped response with IH 4 producing the highest amounts of VEGF. Well accepted as the most potent angiogenesis promoting cytokine, it is clear that the frequency-dependent VEGF production is strongly correlated to the frequency-dependent vessel development. However, considering that no IH condition surpassed the VEGF level produced by the 5%  $O_2$  control, it is evident that other frequency-induced angiogenic factors are at play.

Our data reflects the time-dependent cellular response to hypoxia, in which the balance between pro- and anti-angiogenic

TABLE 1. Experimental oxygenation conditions of varying frequencies.

Condition	Frequency ( $h^{-1}$ )	Total number of cycles	$C_{O_2,high}$ (%)	$t_{O_2,high}$ (min)	$C_{O_2,low}$ (%)	$t_{O_2,low}$ (min)
IH 1	1.8	300	20	7	1	27
IH 2	0.6	100	20	21	1	80
IH 3	0.12	20	20	106	1	398
IH 4	0.06	10	20	212	1	796
IH 5	0.03	5	20	424	1	1591
IH 6	0.012	2	20	1061	1	3978
5%	—	0	5	Constant	—	—

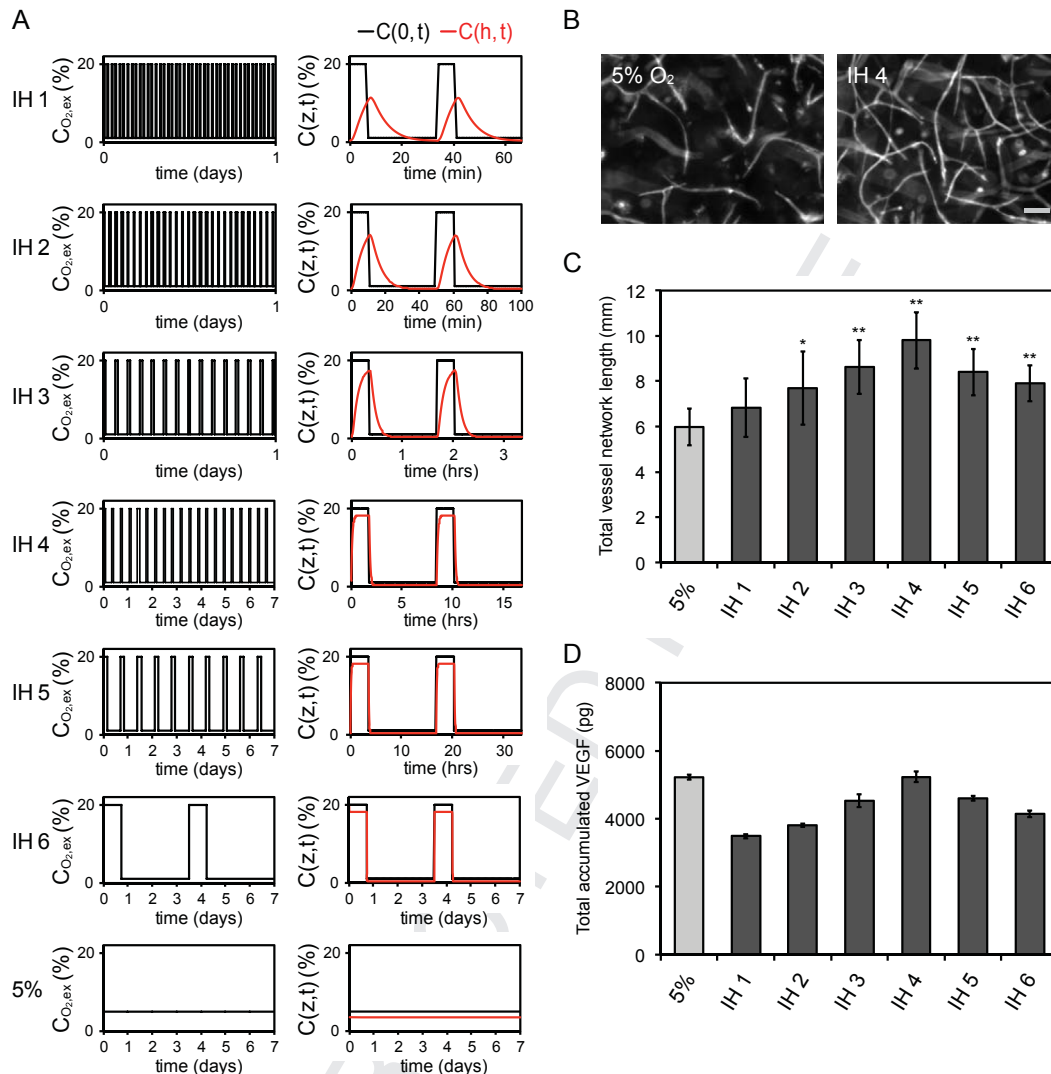


FIG. 2. (A) Experimental oxygenation conditions imposed at the  $z = 0$  boundary are shown as a function of time (black line). Finite element simulations were used to predict the oxygen profile at the base of the tissue (red line). The time lag and dispersion effects are induced by limitations in oxygen diffusion and reaction. (B) Fluorescent images of CD31 labeled endothelial cells show that IH may promote greater vessel network development by the end of the 7-day assay compared to the constant 5%  $O_2$  control. Scale bar represents 100  $\mu m$ . (C) Quantification of total vessel network length demonstrates frequency dependence of IH conditioned tissues. \* $p < 0.05$  and \*\* $p < 0.001$  compared to 5%  $O_2$  control. (D) Total accumulated VEGF in the conditioned tissue samples over the 7-day assay reveal parallel frequency dependence. (For interpretation of the references to color in this figure legend, the reader is referred to the web version of this article.)

mediators is modulated by the severity and duration of hypoxia. Short-term exposure (on the order of minutes to hours) may instigate the post-translational modification of proteins or the activation of pre-existing proteins, most notably the HIF-1 transcription factor (13), leading to VEGF production. Hence, it is likely that the hypoxic exposure ( $t_{O_2,low}$ ) in the higher frequency IH profiles in our study (i.e., approximating IH 1) are sufficient to instigate a corresponding transcriptional response. In contrast, prolonged hypoxic exposure has been shown to lead to endothelial cell death (14); thus, as frequency decreases (i.e., approximating IH 6), the cells may respond in a fashion more similar to chronic hypoxia, which is characterized by cellular stress and damage. Future studies should focus on understanding the expression of angiogenic proteins other than VEGF in response to IH to more fully understand the impact of IH on angiogenesis.

In conclusion, we presented an experimental platform, validated with a computational model, capable of efficiently conferring temporal oxygen control of 3D tissues. We used this system to demonstrate that IH stimulates vessel network formation and VEGF production in a highly correlated fashion that is frequency-

dependent. This work may inform how the vascular tumor micro-environment responds to or modulates IH, and thus provides insight into developing strategies for therapeutic intervention.

This work was supported by the National Institute of Health (grants R01 CA170879 and UH2 TR000481).

## References

- Bergers, G. and Benjamin, L. E.: Tumorigenesis and the angiogenic switch, *Nat. Rev. Cancer*, **3**, 401–410 (2003).
- Baumgardner, J. E. and Otto, C. M.: In vitro intermittent hypoxia: challenges for creating hypoxia in cell culture, *Respir. Physiol. Neurobiol.*, **136**, 131–139 (2003).
- Dewhirst, M. W., Cao, Y., and Moeller, B.: Cycling hypoxia and free radicals regulate angiogenesis and radiotherapy response, *Nat. Rev. Cancer*, **8**, 425–437 (2008).
- Matsumoto, S., Yasui, H., Mitchell, J. B., and Krishna, M. C.: Imaging cycling tumor hypoxia, *Cancer Res.*, **70**, 10019–10023 (2010).
- Hartel, F. V., Holl, M., Arshad, M., Aslam, M., Gunduz, D., Weyand, M., Micoogullari, M., Abdallah, Y., Piper, H. M., and Noll, T.: Transient hypoxia

- induces ERK-dependent anti-apoptotic cell survival in endothelial cells, *Am. J. Physiol. Cell Physiol.*, **298**, C1501–C1509 (2010).
6. **Feron, O., Martinive, P., Defresne, F., Quaghebeur, E., Daneau, G., Crockart, N., Gregoire, V., Gallez, B., and Dessy, C.**: Impact of cyclic hypoxia on HIF-1 alpha regulation in endothelial cells – new insights for anti-tumor treatments, *FEBS J.*, **276**, 509–518 (2009).
  7. **Martinive, P., Defresne, F., Bouzin, C., Saliez, J., Lair, F., Gregoire, V., Michiels, C., Dessy, C., and Feron, O.**: Preconditioning of the tumor vasculature and tumor cells by intermittent hypoxia: implications for anticancer therapies, *Cancer Res.*, **66**, 11736–11744 (2006).
  8. **Chen, X. F., Aledia, A. S., Popson, S. A., Him, L., Hughes, C. C. W., and George, S. C.**: Rapid anastomosis of endothelial progenitor cell-derived vessels with host vasculature is promoted by a high density of cotransplanted fibroblasts, *Tissue Eng. Part A*, **16**, 585–594 (2010).
  9. **Ehsan, S. M., Welch-Reardon, K. M., Waterman, M. L., Hughes, C. C., and George, S. C.**: A three-dimensional in vitro model of tumor cell intravasation, *Integr. Biol. (Camb)*, **6**, 603–610 (2014).
  10. **Zudaire, E., Gambardella, L., Kurcz, C., and Vermeren, S.**: A computational tool for quantitative analysis of vascular networks, *PLoS One*, **6** (2011).
  11. **Ehsan, S. M. and George, S. C.**: Nonsteady state oxygen transport in engineered tissue: implications for design, *Tissue Eng. Part A*, **19**, 1433–1442 (2013).
  12. **Semenza, G. L.**: Targeting HIF-1 for cancer therapy, *Nat. Rev. Cancer*, **3**, 721–732 (2003).
  13. **Semenza, G. L.**: Perspectives on oxygen sensing, *Cell*, **98**, 281–284 (1999).
  14. **Stempien-Otero, A., Karsan, A., Cornejo, C. J., Xiang, H., Eunson, T., Morrison, R. S., Kay, M., Winn, R., and Harlan, J.**: Mechanisms of hypoxia-induced endothelial cell death – role of p53 in apoptosis, *J. Biol. Chem.*, **274**, 8039–8045 (1999).